**THE EUROPEAN
PHYSICAL JOURNAL D**

Regular Article

Beat structure in the solution of scattering problems with nondecaying sources*

Marcelo J. Ambrosio[1,2,5,a], Lorenzo U. Ancarani[3], Antonio I. Gómez[4,5],
Gustavo Gasaneo[4,5], and Darío M. Mitnik[1,2,5]

[1] Instituto de Astronomía y Física del Espacio (IAFE), Universidad de Buenos Aires, C1428EGA Buenos Aires, Argentina
[2] Departamento de Física, Universidad de Buenos Aires, C1428EGA Buenos Aires, Argentina
[3] Théorie, Modélisation, Simulation, SRSMC, UMR CNRS 7565, Université de Lorraine, 57078 Metz, France
[4] IFISUR, Universidad Nacional del Sur, CONICET, Departamento de Física – UNS, Av. L. N. Alem 1253, B8000CPB – Bahía Blanca, Argentina
[5] Consejo Nacional de Investigaciones Cientificas y Tecnicas (CONICET), Buenos Aires, Argentina

Abstract. In this contribution we study mathematical properties of scattering solutions of Schrödinger-type equations with nondecaying, outgoing type, driven terms. We analyze in some details the two-body frame, where an analytical treatment is possible, and find how the scattering solution is expected to contain a beating type structure. The analytical formulation is first presented, and then fully and successfully confirmed with two numerical implementations: the Exterior Complex Scaling and the Generalized Sturmian Functions methods. Our results illustrate the underlying mathematical structure that can be found in, for example, the photoionization of atoms or molecules, in the case when several photons are absorbed or in second order calculations for a single photon absorption. A test case within the three-body frame is also presented, illustrating numerically the presence of beat structures in separately the single and double continuum channels.

1 Introduction

The two-body quantum scattering equation is often discussed in atomic physics textbooks [1,2] considering a right hand side (RHS) composed of a short ranged potential and a stationary wave as an unperturbed (or *prepared*) state. Formal and technical difficulties appear if the potential in the RHS has a Coulomb tail or, worse, if it is a constant value, in combination with a stationary wave. However, if the RHS is composed of a constant value potential times a function with outgoing asymptotic behavior, the problem is well posed, and can be analytically studied and numerically solved as shall be demonstrated here.

As detailed below, in atomic and molecular scattering physics, equations with nondecaying sources may appear. Whether in two or three-body problems, one may be faced with coupled non-homogeneous Schrödinger-like equations with equal or unequal energy. Two features are noteworthy. First, as observed in other similar mathematical/physical situations, the solution of such a system may exhibit beat structures; to our knowledge, this interesting phenomenon has not been discussed previously within scattering studies. Second, the extraction of physical information (i.e. physical observables such as scattering amplitudes and thus, finally, cross sections that can be compared to experimental data) is not at all obvious because the underlying mathematical structure differs from that of the standard scattering theory. The main goal of this article is to study these two features: the presence and characterization of these beating-type structures as well as the extraction of the relevant scattering information. We also support our mathematical findings with numerical examples for two-body and three-body cases. To illustrate the emerging beating-type solutions, we shall use the Generalized Sturmian Functions (GSF) method [3]; thus, a secondary aim of the present paper is to show that GSF, used successfully to solve more traditional scattering problems, can easily solve also situations involving Schrödinger-like differential equations with nondecaying driven terms.

In order to show that such coupled equations see real applications in atomic and molecular physics, consider a general scattering Schrödinger equation $[H - E]\Psi_{full} = 0$; without great restrictions one may assume that $H = H_0 + \lambda W$ where H_0 is a simplified Hamiltonian, W a perturbation and λ is a parameter whose numerical value is finally set to 1. Suppose that the system is in a given initial, prepared, state $\Psi^{(0)}$, of energy E_0, that solves exactly $[E_0 - H_0]\Psi^{(0)} = 0$. As a pure three-body

example, we have electron-hydrogen inelastic scattering, where $\Psi^{(0)}$ would be a continuum state (for the incoming electron) times a bound hydrogen state [4–7]. One way to deal with such problems is to make the ansatz $\Psi_{full} = \Psi^{(0)} + \Psi_{sc}$ [1,8] with Ψ_{sc} containing all the information on the scattering dynamics. The inclusion of the parameter λ associated to W suggests writing the solution as an expansion

$$\Psi_{sc} = \sum_{n=1}^{\infty} \lambda^n \Psi_{sc}^{(n)}. \tag{1}$$

Including also the initial state equation, the successive orders $\Psi_{sc}^{(n)}$ satisfy the following system of differential equations

$$[E_0 - H_0]\Psi^{(0)} = 0, \tag{2a}$$

$$[E_1 - H_0]\Psi_{sc}^{(1)} = W\Psi^{(0)}, \tag{2b}$$

$$[E_2 - H_0]\Psi_{sc}^{(2)} = W\Psi_{sc}^{(1)}, \tag{2c}$$

$$\vdots$$

$$[E_n - H_0]\Psi_{sc}^{(n)} = W\Psi_{sc}^{(n-1)}, \tag{2d}$$

where the notation E_i ($i > 1$) is specified in two examples hereafter.

As a first example, consider an electron scattering problem where W is a sufficiently short-range interaction potential. In this case, for the projectile-target system all energies E_i of equations (2) are equal to the initial total energy E_0. Starting from a known $\Psi^{(0)}$ composed of an incident-projectile momentum eigenstate and a target bound state, the first order scattering equation (2b) for the target subsystem has a driven term (the RHS) that is short ranged because of the bound nature of the initial target state: a scattering solution $\Psi_{sc}^{(1)}$ with pure outgoing behavior can be obtained. One should be able to proceed to the next order equations although they may present some numerical difficulties; indeed, the RHS, $W\Psi_{sc}^{(n-1)}$ ($n \geq 2$), is more spread out in space – and oscillating– since it contains target scattering states, but is still short-ranged because of W. A structurally similar set of equations is found when studying multiphoton ionization by a laser (both types, pulsed and continuous), i.e., with the perturbation coming from the laser instead of an interparticle interaction. Considering up to a two-photon-capture requires the solution of equations (2a)–(2c) with $E_2 \neq E_1 \neq E_0$. The operator W in this physical scenario corresponds to the dipole field. In a recent investigation of the two-photon ionization of hydrogen by a laser pulse [9,10] it was indeed observed that the numerical resolution of the coupled non-homogeneous equations, although feasible, requires special attention. In this case, the finite duration of the pulse ends up shaping a limited-extension RHS. The presented ionization probability showed good agreement with a separate time-dependent calculation. When considering two-photon ionization by a continuous laser source, the RHS is spatially non-vanishing [10]: a beating type second order function ensues, which is more difficult to calculate and to extract ionization amplitudes from.

A two-active-electron example is found in atomic or molecular photoionization by absorption of several successive photons of energy $\hbar\omega$. In the resulting Dalgarno-Lewis driven equations (see, e.g., Refs. [11,12] for two-photon absorption) the E_i are not equal. In equation (2b) $E_1 = \hbar\omega - E_0 - U_p$ (where U_p is the ponderomotive energy), and the dipole operator W acts upon an initial target bound state $\Psi^{(0)}$; the solution $\Psi_{sc}^{(1)}$ corresponding to the ejection of an electron takes outgoing behavior. With an absorption of a further photon, the driven equation (2c), with a different energy $E_2 = 2\hbar\omega - E_0 - U_p$, has a driven term which has an outgoing behavior. By iteration, with absorption of n photons, one searches outgoing solutions to driven equations with energies $E_n = n\hbar\omega - E_0 - U_p$. For such equations the main difficulty lies in the fact that the driven term is not spatially confined, since the long-but-finite nature of the laser is not taken into account, and therefore the RHS continues to contribute at all radial coordinate values. This introduces the same challenges mentioned above for the single-electron analog: first, the scattering wave function numerical calculation requires additional care, and second, the transition amplitude evaluation becomes less clear from an analytical standpoint. The complexities are further stressed due to the inherently more difficult nature of a calculation with two active electrons. Examples of experimental studies have been presented for sequential and nonsequential multiphoton ionization of helium [13,14] and neon [14,15]. Even when the first photon is not energetic enough to produce double continuum, the second order driven term would be nonvanishing for large values of either one electron radial coordinate. The corresponding wave function for these configurations is then expected to contain beating type oscillations.

In order to study the consequences of nonvanishing driven terms that may appear in calculations of real physical two- and three-body problems, we devised some tests, in the form of two coupled equations as (2b)–(2c) with either $E_1 = E_2$ or $E_1 \neq E_2$. The two-body case allows for analytical manipulations and presents the simplest frame on which to expose the underlying mathematical structure. We are aware, however, that two-body problems have lost relevance, presenting little numerical challenge for the computational resources available nowadays. Therefore, we derive here the semi-analytical expressions in the more tractable two-body case, and then proceed with a solely numerical illustration for the more complex three-body frame. Knowledge of the underlying mathematical structure extending to the three-body case can hint more efficient ways of extracting the transition amplitudes from the wave function itself.

For the two-body case, the chosen benchmark we consider is a set of two generalized scattering equations, with one of them depending on the result of the other one. On the left hand side (LHS) of both equations we use the familiar Coulomb potential, since its Green operator expression is known and allows us to carry out analytical studies. The formal solution of the second one involves an integration of a nondecaying integrand. Since that integrand has

outgoing-wave type behavior, the integration can still be performed via an integrating factor as in reference [16]. We obtain semi-analytical results that allow one to observe the emerging nature of the solutions, and we compare and validate them with two alternative numerical approaches. The first one is a two-body Exterior Complex Scaling (ECS) implementation with high order finite differences for arbitrary (real or complex) radial grids. Under the ECS approach [17], the scattering equation is solved using a radial coordinate that lies on the complex plane. Beyond a given radius, the radial coordinate follows a contour that departs from purely real values to the positive half plane, and this reduces any type of outgoing wave to an exponentially damped oscillation. Thus, a zero can be enforced on the solution at the largest radius considered in the calculation, independently of the particular asymptotic energy. The second one is the GSF method [3] which has been proven to be a cost-efficient and adaptable tool to study a variety of single and double continuum collision processes such as electron impact ionization [18–20] and photoionization [21,22]. By numerically solving the proposed benchmark equations, we shall show that GSF may solve scattering problems also with nondecaying driven terms.

Finally, in some future investigation, we intend to use the GSF approach to tackle numerically the inherently more complex three-body problem with nondecaying sources. This would appear, for example, in a second order calculation of the double ionization of helium by fast charge projectiles [18,23–25]. In these references, the system of equations (2a)–(2d) is proposed. For relatively high incident electron energies, the authors solved the first order equation (2b) – which is equivalent to a first order Born approximation – and made a successful comparison with experimental results [26,27]. To investigate electron or proton impact experimental data at lower incident energy regimes (for example, [27,28]), one would need to solve the second order equation (2c), with a nonvanishing driven term. The GSF method has very good scaling properties when extended to the three-body context, requiring comparatively moderate computational resources [22,29]. Here we limit ourselves to the resolution of a coupled system of equations (similar to Eqs. (2b)–(2c)) within a *s*-wave approach of the three Coulomb interactions. As for the two-body case, the second equation contains a driven term with an outgoing type behavior. The GSF method is employed to illustrate numerically that the beat phenomenon can present itself in three-body problems. Since it appears in both single and double continuum channels, the analysis is clearly more intricate.

The outline of the paper is as follows. In Section 2 we define the mathematical problem and provide general analytical expressions for the solution of the two-body driven equation. Section 3 is devoted to show numerical examples using the theory derived in the previous one. We further support those results with two independent numerical approaches. A test three-body case is presented and illustrated numerically in Section 4. Concluding remarks are provided in Section 5.

Atomic units ($\hbar = e = m_e = 1$) are used unless otherwise stated.

2 Statement of the problem

Before giving the set of two non-homogeneous equations we want to explore, let us recall how a driven equation comes about when describing the scattering of two particles of reduced mass μ via a central potential $V_L(r)$. We begin with the stationary Schrödinger equation

$$\left[-\frac{1}{2\mu}\nabla^2 + V_L(r) - E \right]\Psi(\mathbf{r}) = 0, \qquad (3)$$

and use a partial wave decomposition in terms of angular momentum eigenstates:

$$\Psi(\mathbf{r}) = \sum_{l,m} Y_l^m(\hat{\mathbf{r}}) \frac{\psi_l(r)}{r}, \qquad (4)$$

each function $\psi_l(r)$ satisfying the radial equation

$$\left[-\frac{1}{2\mu}\frac{d^2}{dr^2} + \frac{l(l+1)}{2\mu r^2} + V_L(r) - E \right]\psi_l(r) = 0. \qquad (5)$$

For scattering studies, one may split each partial wave $\psi_l(r)$ into two terms [2,30]:

$$\psi_l(r) = \phi_l(r) + \psi_{sc,l}^+(r). \qquad (6)$$

The first, $\phi_l(r)$, is a continuum eigenstate of a given, initial, potential $U(r)$ (e.g., $U(r) = 0$ for a plane wave):

$$\left[-\frac{1}{2\mu}\frac{d^2}{dr^2} + \frac{l(l+1)}{2\mu r^2} + U(r) - E \right]\phi_l(r) = 0. \qquad (7)$$

The scattering function, $\psi_{sc,l}^+(r)$, here taken with outgoing (+) behavior, solves the following driven equation

$$\left[-\frac{1}{2\mu}\frac{d^2}{dr^2} + \frac{l(l+1)}{2\mu r^2} + V_L(r) - E \right]\psi_{sc,l}^+(r)$$
$$= [U(r) - V_L(r)]\phi_l(r) \equiv V_R(r)\phi_l(r), \quad (8)$$

where the label R on the RHS makes it clear that the potential $V_R(r)$ is not the same as the one on the LHS (labelled L). Mathematically, the solution depends very much on the nature of the driven term. In the case of a Coulomb potential $V_L(r)$ and a confined source (any combination of terms written as a power of r times an exponential decay), a detailed study has been presented in reference [31].

In this work we want to investigate the situation with a non-confined source. For this purpose, we consider a system of two coupled driven equations similar to (8):

$$\left[-\frac{1}{2\mu}\frac{d^2}{dr^2} + \frac{l_1(l_1+1)}{2\mu r^2} + V_L^{(1)}(r) - E_1 \right]\psi_{sc,l_1}^{(1)}(r)$$
$$= -V_R^{(1)}(r)\varphi_{l_0}(r), \qquad (9a)$$

$$\left[-\frac{1}{2\mu}\frac{d^2}{dr^2} + \frac{l_2(l_2+1)}{2\mu r^2} + V_L^{(2)}(r) - E_2 \right]\psi_{sc,l_2}^{(2)}(r)$$
$$= -V_R^{(2)}(r)\psi_{sc,l_1}^{(1)}(r), \qquad (9b)$$

each with its energy E_i and angular momentum l_i ($i = 1, 2$). In the first equation, we take $V_R^{(1)}(r)$ that asymptotically acquires a constant value, and the orbital $\varphi_{l_0}(r)$ is short ranged, decaying exponentially. Consequently, $\psi_{sc,l_1}^{(1)}(r)$ reaches its outgoing asymptotic behavior beyond a finite range. In the second one, the orbital is a pure outgoing solution of the first equation, and we consider a nonvanishing $V_R^{(2)}(r)$ that asymptotically also acquires a constant value. Consequently, the scenario for $\psi_{sc,l_2}^{(2)}(r)$ is not the same as for $\psi_{sc,l_1}^{(1)}(r)$, since the driven term in (9b) contains asymptotically an outgoing type function. This fact makes the study of the second driven equation mathematically more difficult, with the asymptotic conditions of $\psi_{sc,l_2}^{(2)}(r)$ not easily determined.

For compactness in the discussions ahead, let us define the whole RHS of equation (9b) as $g(\gamma_1, k_1, r) = -V_R^{(2)}(r) \psi_{sc,l_1}^{(1)}(r)$, while introducing the Sommerfeld parameters $\gamma_i = -Z_i/k_i$ with $k_i = \sqrt{2\mu E_i}$, $i = 1, 2$. We denote

$$\varepsilon^\pm(\gamma, k, r) = e^{\pm i[kr - \gamma \log(2kr)]}, \quad (10)$$

the distorted (eikonal) spherical waves.

In this work we deal with the specific case of a pure Coulomb type $V_L^{(2)}(r) = \frac{Z_2}{r}$, for which the Green operator analytic form is well-known [32,33]:

$$G_{l_2}(r, r') = \frac{2}{W} F_{l_2}(Z_2, k_2, r_<) H_{l_2}^+(Z_2, k_2, r_>), \quad (11)$$

where $r_<$ ($r_>$) indicates the smaller (larger) of r and r'. The Wronskian

$$W = F_{l_2}(Z_2, k_2, r) \frac{dH_{l_2}^+}{dr}(Z_2, k_2, r)$$
$$- H_{l_2}^+(Z_2, k_2, r) \frac{dF_{l_2}}{dr}(Z_2, k_2, r) \quad (12)$$

is coordinate independent [33], and can be evaluated in the asymptotic regime, where the analytical expressions of the regular Coulomb function $F_l(Z_2, k_2, r)$ and the outgoing-type Coulomb function $H_l^+(Z_2, k_2, r)$ are simpler to use.

The formal solution of equation (9b) contains the homogeneous regular solution, $F_l(Z_2, k_2, r)$, plus a non-homogeneous part which can be obtained via the Green operator:

$$\psi_{sc,l_2}^{(2)}(r) = A_0 F_{l_2}(Z_2, k_2, r)$$
$$+ \int_0^\infty G_{l_2}(r, r') g(\gamma_1, k_1, r') dr'. \quad (13)$$

For the purposes of the present investigation we need a function $\psi_{sc,l_2}^{(2)}(r)$ that possesses outgoing flux, i.e., particle emission. Since the Green operator does enforce the proper emissive behavior on the particular solution, any contribution from the regular solution would introduce an unwanted incoming or stationary flux; we therefore set $A_0 = 0$ hereafter. The formalism could be naturally extended to treat stationary components; this, however, goes

beyond the scope of the article. With the Green operator form (11), the integral representing the non-homogenous solution (13) is split into two intervals

$$\psi_{sc,l_2}^{(2)}(r) = \frac{2}{W} H_{l_2}^+(Z_2, k_2, r) \left[\int_0^r F_{l_2}(Z_2, k_2, r') \right.$$
$$\times g(\gamma_1, k_1, r') dr' \right] + \frac{2}{W} F_{l_2}(Z_2, k_2, r)$$
$$\times \left[\int_r^\infty H_{l_2}^+(Z_2, k_2, r') g(\gamma_1, k_1, r') dr' \right]. \quad (14)$$

Let us study the asymptotic behavior of (14). For values of $r > R$, with R large enough, the regular and irregular solutions behave as [34]

$$F_l(Z_2, k_2, r) \xrightarrow{r>R} A_+ \varepsilon^+(\gamma_2, k_2, r) + A_- \varepsilon^-(\gamma_2, k_2, r) \quad (15)$$

$$H_l^+(Z_2, k_2, r) \xrightarrow{r>R} A_H \varepsilon^+(\gamma_2, k_2, r), \quad (16)$$

with $A_\pm$ and A_H complex valued amplitudes that can be easily computed. For the present investigation we consider the case of a strictly outgoing type RHS,

$$g(\gamma_1, k_1, r) \xrightarrow{r>R} A_g \varepsilon^+(\gamma_1, k_1, r). \quad (17)$$

For the range $r > R$, we replace these asymptotic behaviors in (14) and obtain

$$\psi_{sc,l_2}^{(2)}(r) \xrightarrow{r>R} \frac{2}{W} A_H \varepsilon^+(\gamma_2, k_2, r)$$
$$\times \left[\int_0^R F_{l_2}(Z_2, k_2, r') g(\gamma_1, k_1, r') dr' \right.$$
$$+ \int_R^r \left(A_+ \varepsilon^+(\gamma_2, k_2, r') + A_- \varepsilon^-(\gamma_2, k_2, r') \right)$$
$$\left. \times A_g \varepsilon^+(\gamma_1, k_1, r') dr' \right]$$
$$+ \frac{2}{W} [A_+ \varepsilon^+(\gamma_2, k_2, r) + A_- \varepsilon^-(\gamma_2, k_2, r)]$$
$$\times \left[\int_r^\infty A_H \varepsilon^+(\gamma_2, k_2, r') A_g \varepsilon^+(\gamma_1, k_1, r') dr' \right]. \quad (18)$$

We see the appearance of integrals involving the product of two waves $\varepsilon^{s_1}(\gamma_1, k_1, r')$ and $\varepsilon^{s_2}(\gamma_2, k_2, r')$ with s_1 and s_2 taking the values ± 1 (outgoing or incoming type waves, respectively). For convenience we add an exponential decay $e^{-\lambda r}$ (and an arbitrary r power which may come handy if one were to deal with a Coulomb potential $V_R^{(2)}(r)$ on the RHS), and define a class integral which can be worked analytically. The resulting closed form reads:

$$\Theta_{\lambda,p}^{(s_2,s_1)}(\gamma_2, k_2, \gamma_1, k_1, r)$$
$$= \int_r^\infty \varepsilon^{s_2}(\gamma_2, k_2, r') \varepsilon^{s_1}(\gamma_1, k_1, r') r'^p e^{-\lambda r'} dr' \quad (19a)$$
$$= (2k_2)^{-is_2\gamma_2} (2k_1)^{-is_1\gamma_1} r^{1-\nu} E_\nu(\tilde{z}r), \quad (19b)$$

with $\nu = is_2\gamma_2 + is_1\gamma_1 - p$ and $\widetilde{z} = -(is_2k_2 + is_1k_1 - \lambda)$, and involves the exponential integral [35]

$$E_\omega(z) = \int_1^\infty \frac{e^{-zt}}{t^\omega} dt. \tag{20}$$

In terms of these functions, the asymptotic behavior (18) becomes:

$$
\begin{aligned}
\psi_{sc,l_2}^{(2)}(r) \xrightarrow[r>R]{} & \frac{2}{W} A_H \varepsilon^+(\gamma_2, k_2, r) \\
& \times \int_0^R F_{l_2}(Z_2, k_2, r') g(\gamma_1, k_1, r') dr' \\
& + \frac{2}{W} A_H \varepsilon^+(\gamma_2, k_2, r) A_+ A_g \\
& \times \Theta_{0,0}^{(+,+)}(\gamma_2, k_2, \gamma_1, k_1, R) \\
& + \frac{2}{W} A_H \varepsilon^+(\gamma_2, k_2, r) A_- A_g \\
& \times \left[\Theta_{0,0}^{(-,+)}(\gamma_2, k_2, \gamma_1, k_1, R) \right. \\
& \left. - \Theta_{0,0}^{(-,+)}(\gamma_2, k_2, \gamma_1, k_1, r) \right] \\
& + \frac{2}{W} \left[A_- \varepsilon^-(\gamma_2, k_2, r) \right] A_H A_g \\
& \times \Theta_{0,0}^{(+,+)}(\gamma_2, k_2, \gamma_1, k_1, r). \tag{21}
\end{aligned}
$$

For the analysis which follows we require the limiting expressions of $E_\omega(z)$ for small and large argument z [35]:

$$E_\omega(z) \xrightarrow[|z|\to 0]{} \Gamma(1-\omega) z^{\omega-1} - \frac{1}{1-\omega}[1 + \mathcal{O}(z)] \tag{22}$$

$$E_\omega(z) \xrightarrow[|z|\to\infty]{} \frac{1}{z} e^{-z} \left[1 + \mathcal{O}\left(\frac{1}{z}\right)\right], \tag{23}$$

which for $\Theta_{\lambda,p}^{(s_2,s_1)}(\gamma_2, k_2, \gamma_1, k_1, r)$ imply:

$$
\begin{aligned}
\Theta_{\lambda,p}^{(s_2,s_1)}(\gamma_2, k_2, \gamma_1, k_1, r) \xrightarrow[r\to 0]{} & (2k_2)^{-is_2\gamma_2}(2k_1)^{-is_1\gamma_1} \\
& \times \left[\Gamma(1-\nu) \widetilde{z}^{\nu-1} - \frac{r^{1-\nu}}{1-\nu} \right] \tag{24}
\end{aligned}
$$

$$
\Theta_{\lambda,p}^{(s_2,s_1)}(\gamma_2, k_2, \gamma_1, k_1, r) \xrightarrow[r\to\infty]{} \\
- \frac{\varepsilon^{s_2}(\gamma_2, k_2, r) \varepsilon^{s_1}(\gamma_1, k_1, r) e^{-\lambda r} r^p}{is_2k_2 + is_1k_1 - \lambda}. \tag{25}
$$

Notice that for $\lambda = 0$ and $s_1 s_2 = -1$, the two limits do not apply in the $k_1 = k_2$ case.

Assume first that $k_1 \neq k_2$. Making use of the limit for large r, i.e. using (25), we rewrite the asymptotic behavior (21) as

$$\psi_{sc,l_2}^{(2)}(r) \xrightarrow[r\to\infty]{} \mathcal{A}_2^+ \varepsilon^+(\gamma_2, k_2, r) + \mathcal{A}_1^+ \varepsilon^+(\gamma_1, k_1, r), \tag{26}$$

where

$$
\begin{aligned}
\mathcal{A}_2^+ = \frac{2}{W} A_H \Bigg[& \int_0^R F_{l_2}(Z_2, k_2, r') g(\gamma_1, k_1, r') dr' \\
& + A_g A_+ \Theta_{0,0}^{(+,+)}(\gamma_2, k_2, \gamma_1, k_1, R) \\
& + A_g A_- \Theta_{0,0}^{(-,+)}(\gamma_2, k_2, \gamma_1, k_1, R) \Bigg] \tag{27a}
\end{aligned}
$$

$$\mathcal{A}_1^+ = \frac{2}{W} \frac{2ik_2 A_H A_- A_g}{k_2^2 - k_1^2}. \tag{27b}$$

Expression (26) shows clearly that $\psi_{sc,l_2}^{(2)}(r)$ behaves asymptotically as a superposition of two outgoing waves $\varepsilon^+(\gamma_1, k_1, r)$ and $\varepsilon^+(\gamma_2, k_2, r)$, associated to different energies E_1 and E_2 with their respective amplitudes $\mathcal{A}_1^+$ and $\mathcal{A}_2^+$. If we take the limit (25) also with respect to R, $\mathcal{A}_2^+$ simplifies into

$$
\begin{aligned}
\mathcal{A}_2^+ = \frac{2}{W} A_H \Bigg[& \int_0^R F_{l_2}(Z, k_2, r') g(\gamma_1, k_1, r') dr' \\
& + i \frac{A_g A_+}{k_2 + k_1} \varepsilon^+(\gamma_2, k_2, R) \varepsilon^+(\gamma_1, k_1, R) \\
& - i \frac{A_g A_+}{k_2 - k_1} \varepsilon^-(\gamma_2, k_2, R) \varepsilon^+(\gamma_1, k_1, R) \Bigg], \tag{28}
\end{aligned}
$$

which requires only an integration over the non-asymptotic part.

The evaluation of $\Theta_{\lambda,p}^{(+,+)}(\gamma_2, k_2, \gamma_1, k_1, r)$ are performed at radii where the exact Coulomb functions $F_{l_2}(Z_i, k_i, r)$ and $H_{l_2}(Z_i, k_i, r)$ can be matched by weighted $\varepsilon^+(\gamma_i, k_i, r)$ and $\varepsilon^-(\gamma_i, k_i, r)$. From equation (25) it is clear that the functions $\Theta_{0,0}^{(+,+)}(\gamma_2, k_2, \gamma_1, k_1, r)$ behave in a bound, oscillatory, fashion as r grows. The same applies for $\Theta_{0,0}^{(-,+)}(\gamma_2, k_2, \gamma_1, k_1, r)$ which possesses either incoming or outgoing behavior, depending on which momentum is larger.

Let us now consider the delicate case $k_1 = k_2$. The integral $\Theta_{0,0}^{(-,+)}(\gamma_2, k_2, \gamma_1, k_1, r)$ is troublesome since both ν and $\widetilde{z}$ vanish. Clearly divergencies appear in expressions (24) (in the r-independent first term) and in (25). To deal with this situation, we make use of the fact that equation (21) involves the difference

$$
\begin{aligned}
& \Theta_{\lambda,p}^{(s_2,s_1)}(\gamma_2, k_2, \gamma_1, k_1, R) - \Theta_{\lambda,p}^{(s_2,s_1)}(\gamma_2, k_2, \gamma_1, k_1, r) \\
& = (2k_2)^{-is_2\gamma_2}(2k_1)^{-is_1\gamma_1}\left[R^{1-\nu}E_\nu(\widetilde{z}R) - r^{1-\nu}E_\nu(\widetilde{z}r)\right] \\
& \hspace{6cm} (s_2 = -1, s_1 = 1). \tag{29}
\end{aligned}
$$

We then set $k_2 = k_1 + \epsilon$ and take the limit $\epsilon \to 0$ after using (24):

$$
\begin{aligned}
& \Theta_{\lambda,p}^{(s_2,s_1)}(\gamma_2, k_2, \gamma_1, k_1, R) - \Theta_{\lambda,p}^{(s_2,s_1)}(\gamma_2, k_2, \gamma_1, k_1, r) \\
& \hspace{1cm} = (2k_2)^{-is_2\gamma_2}(2k_1)^{-is_1\gamma_1}\left[\frac{r^{1-\nu}}{1-\nu} - \frac{R^{1-\nu}}{1-\nu}\right]. \tag{30}
\end{aligned}
$$

The subtraction played a key role here, cancelling the would-be divergent terms in the limit $\epsilon \to 0$. Setting $p = 0$ and $\lambda = 0$, we have $\nu = 0$ and therefore equation (30) has a linear growth in r. From equation (21) we get the valid description for the asymptotic behavior

$$\psi_{sc,l_2}^{(2)}(r) \xrightarrow[r>R]{} \frac{2}{W} A_H A_- A_g \varepsilon^+(\gamma_2, k_2, r)[r + f(R)], \quad (31)$$

that is to say a well defined solution which oscillates as dictated by $k_1 = k_2$, but grows linearly in amplitude (the r term quickly outgrows the others collected above in $f(R)$). This linear growth would not be present while calculating photoionization by lasers with a single frequency, since the second order energy would be strictly different from the first order one. However, a $k_1 \approx k_2$ situation can be encountered when working numerically in two-photon photoionization with pulses which have a whole distribution of frequencies.

3 Numerical implementations and examples

To illustrate the previous analytical descriptions, we consider now some concrete examples for equation (9b), for which we shall provide the outgoing solution $\psi_{sc,l_2}^{(2)}(r)$. We solve the equation, within a finite domain, with three independent approaches.

The first approach is based on the $\psi_{sc,l_2}^{(2)}(r)$ analytical results outlined in the previous section. For $r > R$, we apply directly equation (26) with (27b) and (28) (when $k_1 \neq k_2$). For $r \leq R$, on the other hand, we rewrite equation (14) as:

$$\psi_{sc,l_2}^{(2)}(r) = \frac{2}{W} H_{l_2}^+(Z_2, k_2, r)$$
$$\times \left[\int_0^r F_{l_2}(Z_2, k_2, r') g(\gamma_1, k_1, r') dr' \right]$$
$$+ \frac{2}{W} F_{l_2}(Z_2, k_2, r)$$
$$\times \left[\int_r^R H_{l_2}^+(Z_2, k_2, r') g(\gamma_1, k_1, r') dr' \right.$$
$$\left. + \int_R^\infty A_H \varepsilon^+(\gamma_2, k_2, r') A_g \varepsilon^+(\gamma_1, k_1, r') dr' \right].$$
$$(32)$$

The integrations involving the exact (nonasymptotic) Coulomb functions $F_{l_2}(Z_2, k_2, r)$ and $H_{l_2}(Z_2, k_2, r)$ are performed numerically. This semi-analytical approach requires knowledge of the regular and irregular solutions of the homogeneous version of equation (9b); for the chosen Coulombic $V_L^{(2)}(r)$, both are well known (for other potentials, both regular and irregular solutions have to be obtained in some other way).

The second method employed in this work is completely numerical in nature. It relies on a high–order finite difference scheme with arbitrary radial grids. For a correct imposition of the, in principle not well established, boundary conditions, the radial grid is chosen to lie on a complex contour. This generates an exponentially damped solution for radii larger than the point of rotation to the complex plane. The implementation profits from the well established capabilities of the ECS method, which has seen many applications within the realm of atomic physics in the past two decades [17].

The third, also numerical, approach is based on the use of GSF [3]. We wish to show that the GSF method, developed within our research group, is a viable option to solve also a not so straightforward two-body challenge, with a nondecaying source. The GSF, noted $S_{nl}(r)$, are eigenfunctions satisfying the following linear, non-homogeneous, equation [3]

$$\left[-\frac{1}{2\mu} \frac{d^2}{dr^2} + \frac{l(l+1)}{2\mu r^2} + \mathcal{U}(r) - E_s \right] S_{nl}(r)$$
$$= -\beta_{nl} \mathcal{V}(r) S_{nl}(r), \quad (33)$$

with β_{nl} the eigenvalues. In equation (33), $\mathcal{U}(r)$ and $\mathcal{V}(r)$ are respectively the auxiliary and generating potentials. The former typically includes the same Coulombic tail of the problem under scrutiny, while the latter dictates the radial domain in which the basis oscillations will be localized. For the present work, we chose a unitary square well type $\mathcal{V}(r)$, vanishing for $r > R_s$. The radius R_s thus defines the radial domain where the basis is linearly independent (beyond R_s all the basis elements are proportional to one another). The energy E_s, though arbitrary, is generally chosen to match the problem energy. This makes for a very efficient basis set, because it matches or approximates the asymptotic conditions of the problem at hand. In the present contribution we use GSF with purely outgoing type asymptotic behavior, noted $S_{nl}^+(r)$, since equation (9b) represents a particle emission. For the solution $\psi_{sc,l_2}^{(2)}(r)$ of this equation, we propose an expansion in terms of such a GSF basis set:

$$\psi_{sc,l_2}^{(2)}(r) = \sum_{n=1}^{N_s} a_{nl_2} S_{nl_2}^+(r). \quad (34)$$

Introducing it into equation (9b) and making use of (33), we are left with:

$$\sum_{n=1}^{N_s} a_{nl_2} \left(V_L^{(2)}(r) - \mathcal{U}(r) - \beta_{nl_2} \mathcal{V}(r) - (E_2 - E_s) \right)$$
$$\times S_{nl_2}^+(r) = -V_R^{(2)}(r) \psi_{sc,l_1}^{(1)}(r). \quad (35)$$

The projection of (35) onto every basis element $S_{n'l_2}^+(r)$ yields a linear system in the, yet to be determined, coefficients a_{nl_2}:

$$\mathbf{Ha} = \mathbf{b}, \quad (36)$$

$$\mathcal{A}_1^+ = \frac{\psi_{sc,l_2}^{(2)}(R_1)\varepsilon^+(\gamma_2, k_2, R_2) - \psi_{sc,l_2}^{(2)}(R_2)\varepsilon^+(\gamma_2, k_2, R_1)}{\varepsilon^+(\gamma_1, k_1, R_1)\varepsilon^+(\gamma_2, k_2, R_2) - \varepsilon^+(\gamma_2, k_2, R_1)\varepsilon^+(\gamma_1, k_1, R_2)}, \tag{39a}$$

$$\mathcal{A}_2^+ = \frac{\psi_{sc,l_2}^{(2)}(R_2)\varepsilon^+(\gamma_1, k_1, R_1) - \psi_{sc,l_2}^{(2)}(R_1)\varepsilon^+(\gamma_1, k_1, R_2)}{\varepsilon^+(\gamma_1, k_1, R_1)\varepsilon^+(\gamma_2, k_2, R_2) - \varepsilon^+(\gamma_2, k_2, R_1)\varepsilon^+(\gamma_1, k_1, R_2)}, \tag{39b}$$

where matrix $\mathbf{H}$ and vector $\mathbf{b}$ elements are given by:

$$\mathbf{H}_{n'n} = \int_0^\infty dr S_{n'l_2}^+(r) \left[V_L^{(2)}(r) - \mathcal{U}(r) \right.$$
$$\left. - \beta_{nl_2}\mathcal{V}(r) - (E_2 - E_s) \right] S_{nl_2}^+(r), \tag{37}$$

$$\mathbf{b}_{n'} = -\int_0^\infty dr S_{n'l_2}^+(r) V_R^{(2)}(r) \psi_{sc,l_1}^{(1)}(r). \tag{38}$$

Notice that the projection is not conjugated [3]. The linear system is solved with the routine ZGESV of the LAPACK library [36].

The calculation of the integrals (37) and (38), requires some special attention. While they are formally defined from zero to infinity, it is common in numerical applications to truncate the integration range at a certain large radius R_s. In our case, since the asymptotic behavior of the integrand is well-known from $R_s > R$ to ∞, the remainder can be integrated analytically using expression (19a). This idea was previously explored by Randazzo et al. [29], where the authors applied it to the overlapping integrals between GSF elements in the case of a three-body problem. In the present work, we needed to use this procedure for both equations (37) and (38). After this analytical tuning, the GSF results were in excellent agreement with the other two methods, as will be seen hereafter.

From expressions (27a) (or its simplified version (28)) and equation (27b), one can evaluate amplitudes $\mathcal{A}_1^+$ and $\mathcal{A}_2^+$ without having to actually calculate $\psi_{sc,l_2}^{(2)}(r)$. The challenge would go no further than the evaluation of a finite range integral and a few eikonals. However, if one wishes to use a given trusted method providing $\psi_{sc,l_2}^{(2)}(r)$, the amplitudes $\mathcal{A}_1^+$ and $\mathcal{A}_2^+$ can be extracted from the following formulae:

see equation (39a) and (39b) above

where the evaluation is made at some given R_1 and R_2 values in the asymptotic regime.

We begin by generating the solution $\psi_{sc,l_1}^{(1)}(r)$ of equation (9a) with the following RHS: we have taken an orbital $\varphi_{l_0}(r)$ being the third Coulomb bound state with zero angular momentum ($l_0 = 0$) and a 2 a.u. core charge, and $V_R^{(1)}(r) = 1$ for all radii. On the LHS we have chosen an energy $E_1 = 2.21$ a.u., an angular momentum $l_1 = 1$, and a Coulomb potential $V_L^{(1)}(r) = -\frac{1}{r}$. The function $\psi_{sc,l_1}^{(1)}(r)$ was obtained with the GSF and ECS approaches alike, the results being numerically identical.

Having $\psi_{sc,l_1}^{(1)}(r)$, we then proceeded with calculating the solution $\psi_{sc,l_2}^{(2)}(r)$ of equation (9b), setting for the purpose $V_R^{(2)}(r) = 1$, $V_L^{(2)}(r) = -\frac{1}{r}$, $E_2 = 3.51$ a.u. and
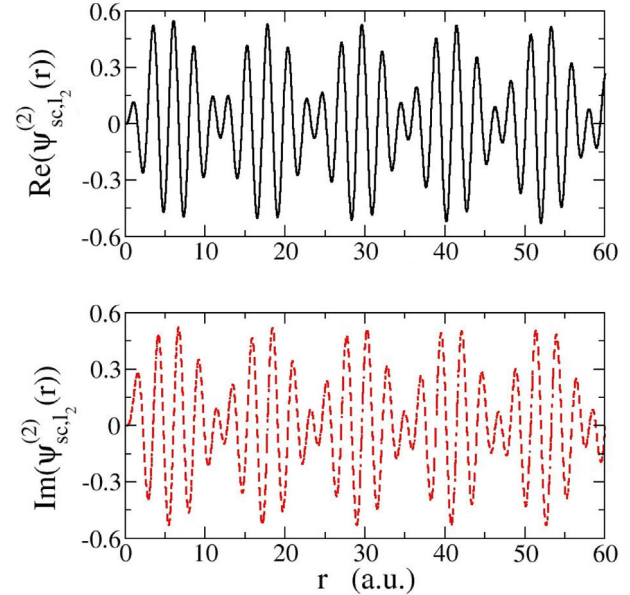

Fig. 1. Real (top panel, solid, black line) and imaginary (bottom panel, dashed, red line) parts of $\psi_{sc,l_2}^{(2)}(r)$ with $E_1 = 2.21$ a.u., $l_1 = 1$, $E_2 = 3.51$ a.u., and $l_2 = 2$. Since GSF, analytical and ECS results are indistinguishable, only the GSF data are shown.

$l_2 = 2$. The three approaches produced indistinguishable scattering functions, so we plotted in Figure 1 only the GSF result obtained with $N_s = 200$ basis functions in a $R_s = 140$ a.u. domain. The solution $\psi_{sc,l_2}^{(2)}(r)$ clearly presents the beating structure, as analytically demonstrated in the previous section, equation (21) and, more explicitly, equation (26).

For consistency, we show in Figure 2 that the semi-analytical scheme produces a continuous function when switching, at $r = 140$ a.u., from expression (32) to the asymptotic one (26) with (27b) and (28). This illustrates the correctness of these expressions and the weights which are in turn closely related to the transition amplitudes. In the figure, we also present an ECS solution with a complex rotation performed at $r = 180$ a.u., which completely agrees with the analytical method. It is worth noting that the ECS method provided an extremely good convergence of the solution with respect to the radius of complex rotation, i.e., in the non-rotated region the solutions were independent of the said radius.

As a final application, we evaluate the potentially most challenging case: coincident energies, i.e., $E_2 = E_1$. This case, according to expression (31), should possess a linearly growing envelope instead of the beating structure
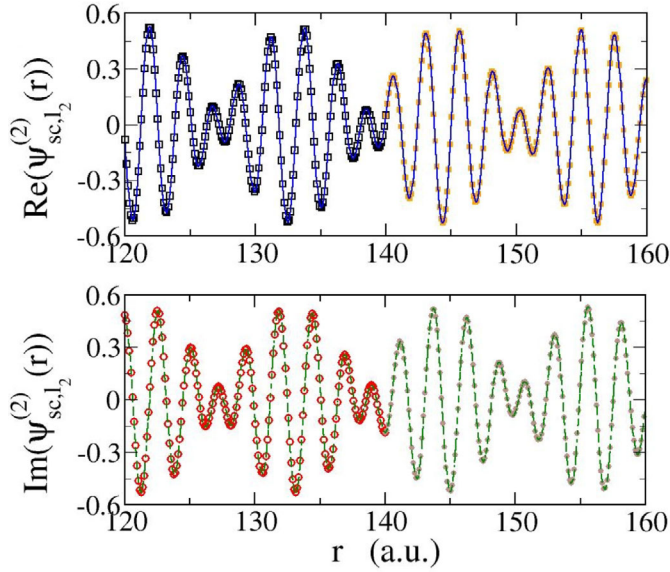
Fig. 2. Real (top panel) and imaginary (bottom panel) parts of the scattering solution $\psi_{sc,l_2}^{(2)}(r)$ for the same parameters as in Figure 1. Here we show only the long range behavior. For the analytical results we used equation (32) up to $r = 140$ (real part: black empty squares, imaginary part: red empty circles), and equation (26) beyond (real part: orange full squares, imaginary part: green full circles). The ECS representation (real part: solid blue line, imaginary part: solid green line) is rotated at $r = 180$ a.u.

depicted in Figure 1. We took $E_2 = E_1 = 2.21$ a.u., keeping the same potentials $V_R^{(2)}(r)$, $V_L^{(2)}(r)$ as well as $\psi_{sc,l_1}^{(1)}(r)$ and $l_2 = 2$. The analytical result, for this energy case strictly based on equation (32), is confirmed by the numerical counterparts (GSF and ECS), all shown in Figure 3; the GSF calculation was performed with 200 basis functions in a $R_s = 60$ a.u. domain. The complete agreement supports both the correctness of the analytical discussion presented in Section 2, and the quality of the GSF and ECS numerical approaches.

The three numerical illustrations confirmed the arguments outlined in the previous section over the asymptotic behavior of the scattering solution $\psi_{sc,l_2}^{(2)}(r)$ of problem (9b), where the driving term is asymptotically an outgoing wave. It is clearly incorrect to assume that we have a pure outgoing wave, unless the source term is spatially confined. The resulting function behaves asymptotically as a superposition of two outgoing waves, dictated by the energies E_1 and E_2 as well as the asymptotic Coulomb part of $V_L^{(2)}(r)$ and $V_L^{(1)}(r)$.

4 Three-body test case

For three-body scattering problems, an analytical study similar to that presented in Section 2 is not feasible, as the Green operator is not known in the whole space. We shall therefore only provide a numerical illustration, considering again a coupled system of equations as (2b) and (2c).
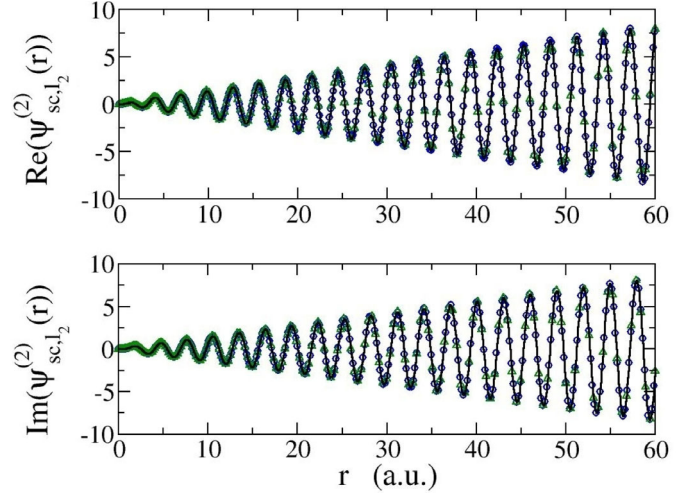

Fig. 3. Real (top) and imaginary (bottom) parts of a scattering solution with $E_2 = E_1 = 2.21$ a.u., $l_2 = 2$. Analytical: black solid line; GSF: blue circles; ECS: green triangles.

They do not correspond to a precise physical problem, but are related to a first and second order calculation of a Temkin-Poet model for the fast projectile double ionization of helium by electronic impact [18]. The first order equation (see Eq. (20) of Ref. [18]) has a bound source containing the target ground state, while the second order will have a driven term involving the first order outgoing solution.

For illustration purposes, we consider the following equations

$$\left[T_2 + T_3 - \frac{Z}{r_2} - \frac{Z}{r_3} + \frac{1}{r_>} - E_1\right] \frac{\Phi_{sc}^{(1)}(r_2, r_3)}{r_2 r_3} = \frac{\phi_0(r_2, r_3)}{r_2 r_3} \tag{40a}$$

$$\left[T_2 + T_3 - \frac{Z}{r_2} - \frac{Z}{r_3} + \frac{1}{r_>} - E_2\right] \frac{\Phi_{sc}^{(2)}(r_2, r_3)}{r_2 r_3} = \frac{\Phi_{sc}^{(1)}(r_2, r_3)}{r_2 r_3}, \tag{40b}$$

where $Z = 2$ is the helium nuclear charge, T_i stand for radial kinetic operators $T_i = -\frac{1}{2r_i^2}\frac{\partial}{\partial r_i}\left(r_i^2 \frac{\partial}{\partial r_i}\right)$, $(i = 2, 3)$, and $r_> = \max[r_2, r_3]$ (as in Refs. [18,19], the target electrons' distances to the nucleus are r_2, r_3). In the first equation we take $E_1 = 10$ eV and $\phi_0(r_2, r_3)$ to be a simple product of ground hydrogenic functions with $Z = 4$ (this non-physical choice allows for a better visualization of the beat phenomenon). In the second equation we take $E_2 = 20$ eV.

To solve (40a) and (40b) we expand both the first and second order scattering functions $\Phi_{sc}^{(j)}(r_2, r_3)$ $(j = 1, 2)$ in terms of a GSF basis

$$\Phi_{sc}^{(j)}(r_2, r_3) = \sum_{n_2, n_3} a_{n_2, n_3}^{(j)} S_{n_2 0}(r_2) S_{n_3 0}(r_3), \tag{41}$$

with the functions $S_{n_2 0}(r_2)$ and $S_{n_3 0}(r_3)$ satisfying the two-body eigenproblem (33). As in our previous work [19,23], we choose generating potentials $\mathcal{V}(r_i)$
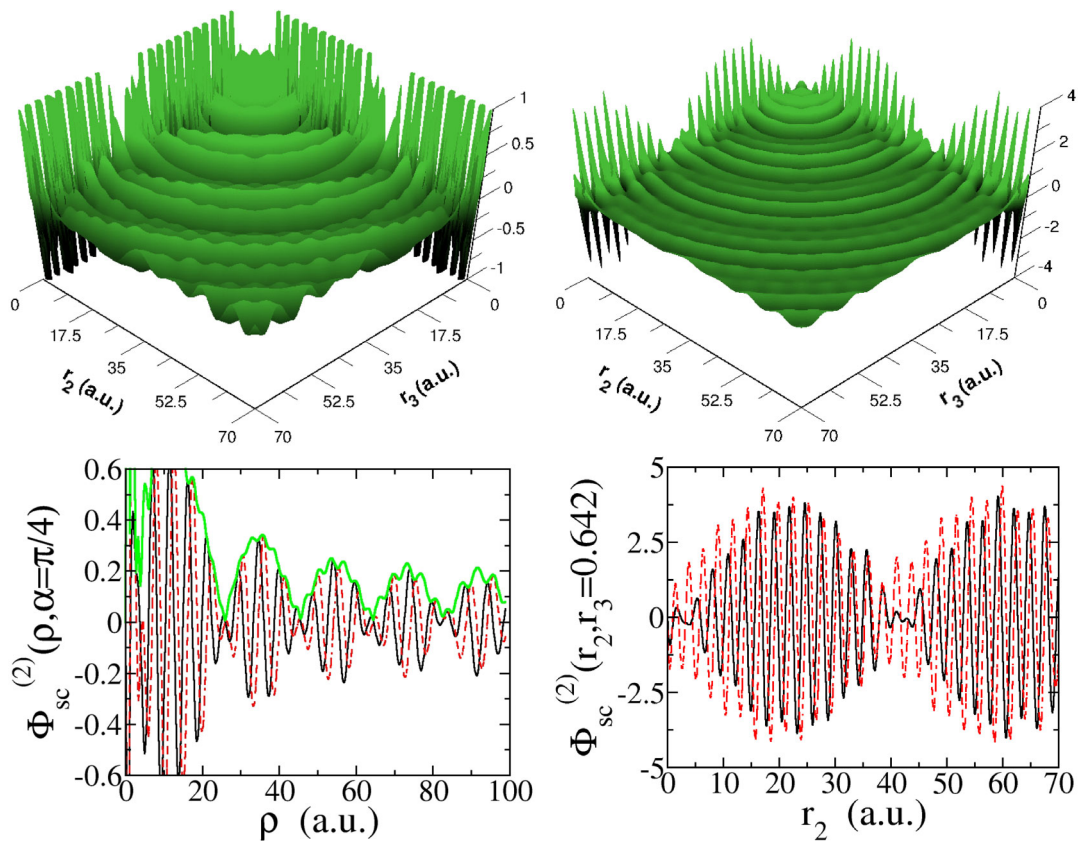
Fig. 4. Top panel: real part of the scattering function $\Phi_{sc}^{(2)}(r_2, r_3)$; the beat structures can be appreciated in the double continuum hyperspherical fronts (left) and in the single ionization components (right). Bottom panel: real (black line) and imaginary (red dashed) parts of $\Phi_{sc}^{(2)}(r_2, r_3)$ for: (left) a fixed hyperangle $\alpha = \pi/4$ cut; (right) a fixed radius $r_3 = 0.642$ a.u. To guide the eye, in the hyperspherical case we also depict the modulus as the (green) enveloping curve.

of the square-well type for both r_2 and r_3, and pure Coulomb auxiliary potentials $\mathcal{U}(r_i)$. Equations (40a) and (40b) are converted into a linear system in the expansion coefficients $a_{n_2,n_3}^{(j)}$ after replacing (41) and projecting onto every product $S_{n_2'0}(r_2) S_{n_3'0}(r_3)$; the reader can find more details on the use and qualities of the GSF applied to three-body problems in reference [3].

The solution $\Phi_{sc}^{(1)}(r_2, r_3)$ calculated with the GSF method is determined with a hyperspherical outgoing behavior, which describes the electronic double continuum (this is not shown here, but can be appreciated in $(e, 3e)$ calculations in either the physical case [23] or in a s-wave model [18]); for small values of either r_2 or r_3, $\Phi_{sc}^{(1)}(r_2, r_3)$ contains the single continuum channels. The solution $\Phi_{sc}^{(2)}(r_2, r_3)$ of the second equation (40b), which contains now a pure outgoing function, is shown as a function of r_2 and r_3 in the top panel of Figure 4; the left panel allows visualizing the beat structure for the double continuum channel while the right panel (note the different scale) allows to see the phenomenon in the single ionization channels.

The bottom panels of Figure 4 show details of the beat phenomenon through cuts of both the real and imaginary parts of $\Phi_{sc}^{(2)}(r_2, r_3)$. To describe the double continuum hy-

perspherical coordinates $\rho = \sqrt{r_2^2 + r_3^2}$ and $\tan \alpha = r_3/r_2$ are more suitable. The cut along the diagonal $r_2 = r_3$, i.e., on a fixed hyperangle $\alpha = \pi/4$, clearly illustrates the beat structure in the hyperradius ρ (left panel). The observed beating envelope wavelength is in good agreement with the expected 18.2 a.u., determined solely by the energies E_1 and E_2. In the right panel, $\Phi_{sc}^{(2)}(r_2, r_3)$ is shown for fixed value $r_2 = 0.642$ a.u. When either r_2 or r_3 are small, the single continuum channels acquire a very significant amplitude. It is in these regions that the application of the two-body analysis of Section 2 is applicable, yet at the same time more intricate in the sense that many single ionization channels are added up [19]. The most dominant and clearly visible single continuum channel corresponds to ionization without excitation, easily identified by its rapid oscillations. The calculated wavelength (39.6 a.u.) for the enveloping beat structure (it is related to the chosen energies E_1, E_2, and also that of the He$^+$ ground state) matches the one observed in the figure. To sum up, Figure 4 clearly shows that beat structures are present in both channels. The mathematical analysis is more intricate for the three-body case as one should investigate the asymptotic regimes of the three-body Green operator in each channel. However, even from a numerical solution like the one presented in Figure 4, the evaluation

of the wave function at a given hyperangle α lends itself to a subsequent reexpansion in terms of two GSF basis sets (with energies E_1 and E_2) in ρ, multiplied by the decay factor $\rho^{-1/2}$. This procedure (currently an interest of our investigation) can be a vehicle to easily obtain, for a given energy sharing, the transition amplitudes, as in references [18,23,24], for the two energy components.

The scattering function depicted in Figure 4 contains by design the complexity of a driven term with hyperspherically outgoing waves. If, in contrast, the first order solution should not present such a hyperspherical front, then the beating structures would be expected to appear only for small values of either r_2 or r_3 coordinates. This extends to below-threshold sequential double photoionization calculations corresponding to the experiments discussed in references [13–15], where the first photon is only able to excite up to single continuum states. The second order driven term therefore does not enforce hyperspherical beats on the solution, and the beating structures can only exist on the single continuum contributions, localized where either r_2 or r_3 is small. The double continuum information in these cases can be extracted by the methods shown in references [18,19,23,24].

5 Concluding remarks

In this article we presented the mathematical and theoretical background which is to be found in two-body scattering-like problems when the driven term behaves asymptotically as a pure outgoing wave. Contrary to the case when the source is spatially confined, one does not find a pure outgoing wave.

For the two-body case, we proposed a coupled system of driven equations, we studied analytically the expected solution and obtained its asymptotic behavior. The solution was shown to contain a beating structure, dictated by the energies of the two equations and by the oscillations of the driven term of the second one. The analysis is supplemented with numerical examples; full agreement is found between the results obtained with the derived formulae, an ECS implementation and a GSF approach. We focussed on three aspects with an example for each. In the first one we verified that the beating structures do appear, and are corroborated by all the considered resolution methods. The second example shows that the asymptotic simplifications of the complete analytical expression are correct. These results should be useful at the moment of extracting the transition amplitudes of a given physical scattering problem, as in the field of photoionization of atoms [9,10] or molecules [21]. The final example consists of a potentially conflictive situation where the same energy is taken for the two equations. A linear enveloping growth is observed, as expected from the equal energy limit in the analytical expressions. The characterization of the resulting wavefunction would be by itself interesting, but for practical purposes it is equally important to be able to extract the transition matrix information. We provide explicit formulae to extract the relevant amplitudes for both energy components involved, stemming directly from our analytical formulation. These expressions can be used even without having the driven equation fully solved, as it requires only some details about the driven term. Besides, we also give another expression tailored to extract the amplitudes from an already calculated wavefunction.

Going beyond the two-body case, applications to a second order calculation for double ionization of helium by electron impact are envisaged; in this case, the three-body scattering equation has a driven term containing an hyperspherical outgoing wave. A full analytical treatment similar to the one presented in this contribution is then extremely complicated, if not impossible. However, beat structures are illustrated here with a simplified *s*-wave system of coupled equations. The numerical resolution through the GSF method in spherical coordinates allowed us to show them in both the single and double continuum channels, each with its expected wavelength. For the double continuum, the more adequate hyperspherical coordinates [3] should help for a deeper investigation. The fact that the hyperspherical beat structure is generated by the superposition of wave fronts (also hyperspherical) with energies E_1 and E_2 can be analyzed via an energy eigenstate decomposition. This should in turn lead to a way of extracting the transition amplitude from this intricate scattering function, and is the subject of our current investigations.

Author contribution statement

We arrange the manuscript contributions into three main categories, concerning the analytical studies and physical interpretation, numerical implementations and the writing of the current manuscript. The order reflects the relative additions by each author to the given item:

- analytical studies/physical interpretation: Ambrosio, Ancarani, Gómez, Gasaneo;
- numerical implementations: Ambrosio, Gómez, Mitnik;
- writing process: Ancarani, Ambrosio.

References

1. B.H. Bransden, C.J. Joachain, *Physics of atoms and molecules* (Englewood Cliffs, NJ, Prentice-Hall, 2003)
2. R.G. Newton, *Scattering Theory of Waves and Particles*, 2nd edn. (Dover Publications, 2002)
3. G. Gasaneo, L.U. Ancarani, D.M. Mitnik, J.M. Randazzo, A.L. Frapiccini, F.D. Colavecchia, Adv. Quant. Chem. **67**, 153 (2013)
4. I. Bray, J. Phys. B **32**, L119 (1999)

5. I. Bray, Phys. Rev. Lett. **89**, 273201 (2002)
6. C.W. McCurdy, T.N. Rescigno, D. Byrum, Phys. Rev. A **56**, 1958 (1997)
7. S. Jones, A.T. Stelbovics, Phys. Rev. Lett. **84**, 1878 (2000)
8. I. Bray, D.V. Fursa, A.S. Kadyrov, A.T. Stelbovics, A.S. Kheifets, A.M. Mukhamedzhanov, Phys. Rep. **520**, 135 (2012)
9. A.I. Gómez, G. Gasaneo, D.M. Mitnik, J. Phys.: Conf. Ser. **635**, 092123 (2015)
10. A.I. Gómez, G. Gasaneo, D.M. Mitnik, M.J. Ambrosio, L.U. Ancarani, Eur. Phys. J. D **70**, 207 (2016)
11. D.A. Horner, F. Morales, T.N. Rescigno, F. Martín, C.W. McCurdy, Phys. Rev. A **76**, 030701(R) (2007)
12. D. Horner, C. McCurdy, T. Rescigno, Phys. Rev. A **78**, 043416 (2008)
13. H. Hasegawa, E.J. Takahashi, Y. Nabekawa, K.L. Ishikawa, K. Midorikawa, J. Phys. A **71**, 023407 (1992)
14. A. Rudenko, L. Foucar, M. Kurka, Th. Ergler, K.U. Kühnel, Y.H. Jiang, A. Voitkiv, B. Najjari, A. Kheifets, S. Lüdemann, T. Havermeier, M. Smolarski, S. Schössler, K. Cole, M. Schöffler, R. Dörner, S. Düsterer, W. Li, B. Keitel, R. Treusch, M. Gensch, C.D. Schröter, R. Moshammer, J. Ullrich, Phys. Rev. Lett. **101**, 073003 (2008)
15. A.A. Sorokin, M. Wellhöfer, S.V. Bobashev, K. Tiedtke, M. Richter, Phys. Rev. A **75**, 051402(R) (2007)
16. M.J. Ambrosio, J.A. Del Punta, K.V. Rodriguez, G. Gasaneo, L.U. Ancarani, J. Phys. A **45**, 015201 (2012)
17. C.W. McCurdy, M. Baertschy, T.N. Rescigno, J. Phys. B **37**, R137 (2004)
18. G. Gasaneo, D.M. Mitnik, J.M. Randazzo, L.U. Ancarani, F.D. Colavecchia, Phys. Rev. A **87**, 042707 (2013)
19. M.J. Ambrosio, G. Gasaneo, F.D. Colavecchia, Phys. Rev. A **89**, 012713 (2014)
20. M.J. Ambrosio, L.U. Ancarani, D.M. Mitnik, F.D. Colavecchia, G. Gasaneo, Few-Body Syst. **55**, 825 (2014)
21. C. Granados-Castro, L. Ancarani, G. Gasaneo, D. Mitnik, Few-Body Syst. **55**, 1029 (2014)
22. J.M. Randazzo, D. Mitnik, G. Gasaneo, L.U. Ancarani, F.D. Colavecchia, Eur. Phys. J. D **69**, 189 (2015)
23. M.J. Ambrosio, F.D. Colavecchia, G. Gasaneo, D.M. Mitnik, L.U. Ancarani, J. Phys. B **48**, 055204 (2015)
24. M.J. Ambrosio, D.M. Mitnik, L.U. Ancarani, G. Gasaneo, E.L. Gaggioli, Phys. Rev. A **92**, 042704 (2015)
25. M.J. Ambrosio, D.M. Mitnik, A. Dorn, L.U. Ancarani, G. Gasaneo, Phys. Rev. A **93**, 032705 (2016)
26. D. Fischer, R. Moshammer, A. Dorn, J.R. Crespo López-Urrutia, B. Feuerstein, C. Höhr, C.D. Schröter, S. Hagmann, H. Kollmus, R. Mann, B. Bapat, J. Ullrich, Phys. Rev. Lett. **90**, 243201 (2003)
27. A. Dorn, A. Kheifets, C.D. Schröter, B. Najjari, C. Höhr, R. Moshammer, J. Ullrich, Phys. Rev. A **65**, 032709 (2002)
28. A. Lahham-Bennani, A. Duguet, M.N. Gaboriaud, I. Taouil, M. Lecas, A.S. Kheifets, J. Berakdar, C. Dal Cappello, J. Phys. B **34**, 3073 (2001)
29. J.M. Randazzo, F. Buezas, A.L. Frapiccini, F.D. Colavecchia, G. Gasaneo, Phys. Rev. A **84**, 052715 (2011)
30. C.J. Joachain, *Quantum Collision Theory* (American Elsevier Publishing Co., Inc., 52 Vanderbilt Ave., New York, 1975)
31. G. Gasaneo, L.U. Ancarani, Phys. Rev. A **82**, 042706 (2010)
32. A.D. Alhaidari, E.J. Heller, H.A. Yamani, M.S. Abdelmonem, *The J-matrix Method: Developments and Applications*, 1st edn. (Springer, 2008)
33. H.A. Yamani, L. Fishman, J. Math. Phys. **16**, 410 (1975)
34. W.R. Johnson, *Atomic Structure Theory: Lectures on Atomic Physics* (Springer-Verlag, 2007)
35. *Exponential integral e – from wolfram mathworld*, `http://mathworld.wolfram.com/En-Function.html`
36. *Lapack – linear algebra package*, `http://www.netlib.org/lapack/`